RSC Advances

ROYAL SOCIETY OF CHEMISTRY

www.rsc.org/advances

Incorporation of silica particles into decellularized tissue biomaterial and its effect on the macrophage activation

Birzabith Mendoza-Novelo[a,*], María C. Lona-Ramos[a], Gerardo García-González[b], Laura E. Castellano[c], Jorge Delgado[a], Patricia Cuellar-Mata[d], J. Mauricio Flores-Moreno[e], Juan Vargas[f], J. Alfredo Gutiérrez[b], Eva E. Ávila[d], José L. Mata-Mata[b]

[a] Depto. de Ingenierías Química, Electrónica y Biomédica, DCI, Universidad de Guanajuato, Loma del Bosque 103, 37150, León, México

[b] Depto. de Química, DCNE, Universidad de Guanajuato, Noria alta s/n, 36050, Guanajuato, México

[c] Depto. de Ciencias Aplicadas al Trabajo, DCS, Universidad de Guanajuato, Garza Sada 532, 37150, León, México

[d] Depto. de Biología, DCNE, Universidad de Guanajuato, Noria alta s/n, 36050, Guanajuato, México

[e] Centro de Investigación en Óptica A. C., Loma del Bosque 115, 37150, León, México

[f] IPN-Unidad Profesional Interdisciplinaria de Ingenierías Campus Guanajuato, Industrial Puerto interior, 36275, Silao de la Victoria, México

*Correspondence: b.mendozanovelo@ugto.mx, Phone: +52-477-7885100 ext 8464

Abstract

This paper describes an optimized procedure to incorporate silica particles by hydrolysis/polycondensation of sodium silicate into pericardial (ECM) matrix scaffolds and points out the effect of the biocomposites on the *in vitro* response of macrophages by assessment the secretion of signaling molecules. Variables (concentration, pH, time) of the sol-gel process allow a gradual incorporation of silica into the ECM scaffolds as confirmed by gravimetry, FT-IR, SEM and EDX microanalysis. The SiO_2 incorporation increases the resistance to *in vitro* degradation but not alters either denaturation temperature or free amines of non-crosslinked ECM fibrous scaffolds, however, properties of oligourethane-crosslinked scaffolds are not modified after silica incorporation. Despite the fact that cell viability is gradually decreased on the ECM materials crosslinked with oligourethane and functionalized with silica, murine RAW264.7 macrophages are able to secrete b-FGF, TGF-β1 and VEGF. Secretion of growth factors by RAW264.7 macrophages after 6 h of culture on scaffolds containing silica was lower but it was sustained for 24 h as compared to cells cultured on silica-free materials. Human peripheral blood macrophages cultured with materials containing silica show a higher production of IL-6, IL-10 or TNF-α than with the silica-free counterparts but in a time-dependent manner from one to four days of culture. Results suggest that stimulation of macrophages is induced by silica particles deposited onto the ECM fibrous network, which represents an opportunity to control the cell response to decellularized tissue-derived biomaterials through strategies intended to stimulate cells via signaling molecules secreted by macrophages.

Keywords: crosslinked/decellularized scaffolds; silica functionalization; macrophage activation

1. Introduction

Crosslinking and functionalization of extracellular matrix (ECM) scaffolds derived from animal tissues are strategies intended to tailor the physicochemical properties and ultimately to improve its biological performance in tissue engineering applications. Crosslinking of collagen, main component of matrices as dermis or pericardium, is a first action to slow or prevent its degradation, to inhibit the recognition of surface epitopes by the host, and to improve mechanical properties.[1-2] Our research group has reported a method in which collagen is crosslinked through isocyanate reactions with water-soluble blocked urethane oligomers after pH-responsive deblocking of carbamoylsulfonate end groups. This method allowed the preparation of a porous collagen mesh coated with oligourethanes that reveals excellent tensile mechanical properties and a degree of crosslinking adjusted tuning pH, volume, concentration or molecular weight.[3-4] Furthermore, effective stabilization of biological scaffolds with oligourethanes can be achieved simultaneously with incorporation of silica by the sol-gel process of tetraethyl orthosilicate.[5] Thus, although silica is generally accepted as having low toxicity, the biocompatibility of silicon and silica in its different forms (i.e. nanoparticles, gels, films) as a "new" class of biomaterial should be revisited.[6]

Silicate–biopolymer hybrids manufactured in different forms have recently received considerable attention as templates to repair/replace bone-defective tissue [7-8], to induce osteoblastic differentiation [9-13], to treat chronic wounds [14], to immobilize cells [15-16], to delivery drug [17-21] and morphogenetic proteins [22-23], and to trigger cell-mediated immunity for tumor immunotherapy. [24-25] The incorporation of silicate particles into biopolymers has shown that yields a controllable biodegradability through adjustment of the silicate content [26-27], and that influence the cell response through intracellular uptake of the silicate particles and its dissolution products. The nanoparticulate debris released from biomaterials containing silicon can reach and penetrate the cell surface affecting its behavior in a manner that dependent of size/porosity, surface chemistry (e.g. ≡Si-OH group concentration, charge) and dissolution

(biodegradation) rate. [28-33] This is the case of fibroblasts that are internalized by aggregates of silica nanoparticles, which are dissolved intracellularly and released either as colloidal or soluble species.[34-36] Key aspects in tissue engineering issues such as osteogenic differentiation of stem cells [10,12] and enhanced angiogenesis [35] have shown be improved by the degradation products of biomaterials containing silicon.

Macrophages are immune cells key players in the release of messengers and mediators (e.g. enzymes, cytokines and growth factors) that act as signals to induce migration, proliferation or differentiation of other cell types. [37] Macrophages mediate the healing responses to implanted biomaterials, fundamentally by two outcomes: scar tissue formation (M1 pathway) or regeneration (M2 pathway). [37-38] The modulation of the inflammatory response by the physical and chemical properties of scaffolds represents a hypothesis currently assessed in the design of biomaterials. For instance, mechanical strain [39], glycoprotein adsorption [40] and chemical composition [41-43] are some aspects related to biomaterial that are keys to modulate the translation of human peripheral blood-derived macrophages from a pro-inflammatory process (M1) to an anti-inflammatory process (M2). Recent reports have described the engagement of cytokines secreted by macrophages in angiogenesis and neovascularization in co-cultures on both 2D [44] and 3D [45] (on collagen templates). Thus, pro-inflammatory stimuli have been proposed as an active participant in the hard and soft tissue engineering context to accelerate healing mechanisms. [44]

The stimulation of macrophages to secrete signaling molecules able to contribute to tissue repair process could be achieved on (crosslinked or non with oligourethane) ECM templates containing silica. In this study we prepared biocomposites consisting of decellularized pericardial ECM scaffolds with/without silica particles to evaluate the *in vitro* response of macrophages by assessing the secretion of growth factors and signaling molecules. The particulate silica was incorporated into the non-crosslinked and oligourethane-crosslinked ECM templates using sodium silicate (Na_4SiO_4) and a sol-gel process. The

viability of fibroblasts, RAW264.7 macrophages and human peripheral blood-derived macrophages, and the production of IL-6, IL-10, TNF-α, b-FGF, TGF-β1 and VEGF by macrophages were evaluated.

2. Experimental Section

2.1. Materials

Acellular pericardial ECM scaffold - Biological scaffolds were prepared by decellularization of bovine pericardial tissue using a method that combines reversible alkaline swelling and the use of a non-ionic detergent.[46] Briefly, samples were placed in distilled water (4°C, 18 h) containing calcium oxide (0.8w%) and Triton X-100 (1w%). Afterwards, they were stirred (2x, RT, 20 min) in a solution containing ammonium sulphate (2%) and subsequently stirred (RT, 24 h, 20 rpm orbital agitation) in sterilized PIPES buffered saline solution (PiBS, 30 mM, 0.9% NaCl, pH 7.4) containing Triton X-100 (1w%) and finally washed with PiBS. At the end, samples were incubated in a solution of nucleases (10 mM Tris–HCl, pH 7.6, 2.5 mM $MgCl_2$, 0.5 mM $CaCl_2$ containing 0.2 mg mL^{-1} of DNase and 0.02 mg mL^{-1} of RNase) and washed (2x, RT, 15 min, 100 mM Tris, pH 8, 30 mM EDTA).

Urethane oligomer crosslinker - The oligourethane was synthesized as previously described elsewhere.[5] Briefly, poly(ethylene glycol) (Mw 1000 g mol^{-1}) reacted with hexamethylene diisocyanate in a molar NCO:OH ratio of 4.0:1.0 for 2 h at 100°C. In a second step, sodium bisulphite (40w% solution in water) was added in the prepolymer and the reaction continued at 40°C by 2 h. Finally, the solution was diluted with water to give a product of water-soluble blocked oligourethane.

Oligourethane-crosslinked ECM scaffolds - Pericardial ECM scaffold samples were crosslinked with oligomers as follows:[4] Hydrated samples of known mass were immersed in PiBS at a 1:5 (w/w) scaffold:PiBS, then oligourethane (15w%) was added and the mixture was stirred (RT, 2 h, 20 rpm). In a second step, magnesium oxide (0.4w%) was added and the crosslinking reaction extended (22 h, 20 rpm). Finally, samples were washed with distilled water and saline solution to remove residual reagents.

Other materials – 3-(4,5-dimethylthiazol-yl)-2,5-diphenyltetrazolium bromide (MTT), 2,4,6-Trinitrobencensulphonic acid (TNBS) and collagenase type I (288 U/mg solid, *Clostridum histolyticum*) were acquired from SigmaAldrich (Mexico).

2.2. Incorporation of silica into the scaffolds

Non-crosslinked or oligourethane-crosslinked ECM scaffold samples were functionalized with silica as follows: Hydrated samples were immersed in a solution of sodium silicate (Na_4SiO_4, 0.33 M, pH 7, neutralized with HCl 1 M) under stirring (RT, 30 min). Finally, samples were washed with distilled water (4x) and lyophilized. In preliminary assays, concentration (0.33, 0.5 and 1 M), time (15, 30, 60 and 120 min) and pH (6, 7 and 8) of hydrolysis-condensation reaction of sodium silicate was optimized in terms of the amount of silica incorporated into the ECM scaffolds (see Fig. S1) and the collagenase degradation resistance (see Fig. S2).

2.3. Composition and microstructure evaluation of biocomposite scaffolds

Gravimetry – Hydrated samples (10 x 10 mm) were weighted and then dried in an oven at 60°C until weight was constant. Then, samples were heated in an oven at 800°C during 2 h. The remaining inorganic mass was registered. Finally, content of water, ECM material or oligourethane/ECM material and silica was calculated.

FT-IR – Infrared spectroscopy information of the silica-functionalized ECM scaffolds was obtained using the ATR technique on a Nicolet iS50 FT-IR Spectrometer. The materials were dehydrated in ethanol and dried in an oven at 30°C under vacuum. The dry samples were analyzed on the diamond crystal and ATR-FTIR spectra, averaging 32 scans, were recorded at 4 cm^{-1} of resolution from 4000 to 650 cm^{-1}.

SEM and EDX microanalysis - The morphology of scaffolds covered with gold was observed by low-vacuum scanning electron microscopy (SEM, JEOL, JSM 6360LV or FESEM 7600F). Using an EDX analyzer coupled to the scanning electron microscope, the elemental composition of calcination-remaining inorganic material was obtained.

2.4. Assessment of crosslinking, stability and water uptake of biocomposite scaffolds

DSC - Thermal transitions were evaluated by differential scanning calorimetry (Diamond DSC calorimeter, Perkin Elmer). Approximately 5 mg of hydrated samples were heated from 40 to 100°C with a heating rate of 10°C min^{-1}. Results from the first scan were used to report thermal properties of the ECM scaffolds.

Blocked matrix-amines - The extent or degree of crosslinking was also evaluated by the change in the free amine content in materials by means of the TNBS assay. Samples of known mass (5 x 5 mm) were conditioned in $NaHCO_3$ (4.0%, 2 mL, 30 min) and then were reacted with TNBS (0.5w%, 1 mL, 40 °C, 2 h). Subsequently, samples were washed (4x) with NaCl (0.9w%) and then hydrolyzed in HCl (25%, 1 mL, 60 °C). The hydrolyzate was diluted to 5 mL and the absorbance at 344 nm was measured. The amine group concentration was reported in mmol per gram of dry scaffold sample (molar absorption coefficient14,600 mL $mmol^{-1}$ cm^{-1}).

Resistance to degradation and water uptake - The resistance to the *in vitro* degradation was studied under enzymatic (125 μg mL^{-1} of type I collagenase, 50 mM Tris•HCl, pH 7.4, 0.03w% NaN_3, 5 mM $CaCl_2$•$2H_2O$) or non-enzymatic (DMEM medium) conditions. ECM scaffold samples of known mass (5 x 10 mm) were incubated in the degradation solution (1 mL, 37°C) under orbital stirring with change of solution every three days. Finally, the mass loss was calculated gravimetrically.

2.5. Assessment of *in vitro* cellular response to biocomposite scaffolds

Cytotoxicity test – Primary culture of rat dermal fibroblasts or mouse macrophage cells (RAW264.7) were routinely grown in DMEM or RPMI-1640 (Gibco®) medium supplemented with fetal bovine serum (FBS, 10%, Gibco®). Lyophilized ECM scaffolds (5 x 5 cm) were sanitized in an ethanol/peracetic acid (4%/0.1%) solution (RT, 2 h), sterile PBS (3x) and UV radiation (2 h), and then plated in 96-well microplates. Cells suspended in 200 μL were plated at $5x10^4$ cells per well containing samples and then cultured (10% FBS, 37°C, 5% CO_2, 95% humidity) for 24 h. The viability of macrophages or fibroblasts was quantified by MTT on scaffold samples and on wells. For this, after culture, scaffolds were transferred to empty wells and 20 μL of MTT solution was added to remaining polystyrene wells and scaffold-containing wells. Cells were maintained under these conditions for 3 h, then the medium was decanted, cells were washed and the blue formazan crystals were dissolved in 2-propanol and finally optical density of the supernatants was measured at 540 nm. The absorbance of MTT reduced by cells cultured on wells (without ECM scaffolds) represented the 100% of cell viability. In addition, morphology of adherent cells on scaffold fixed with 4% paraformaldehyde and covered with gold was examined with the scanning electron microscope JEOL JSM 6360LV.

Quantification of growth factors secreted by RAW264.7 macrophages – ECM scaffolds (disks 15 mm) were sanitized, as described previously, and plated in wells of 24-well microplates. Cells suspended in 1000 μL of RPMI medium supplemented with 10% FBS and antibiotics (50 μg mL^{-1} penicillin/streptomycin) were plated at $1x10^5$ per well containing samples and then cultured (37°C, 5% CO_2, 95% humidity) during 6 or 24 h. After that time, the medium was collected to quantify growth factors. Quantification of the growth factors TGF-β1, b-FGF and VEGF was performed using ELISA kits (Invitrogen™) according to specifications. The number of viable macrophages on the scaffolds and on the rest of the surface of the wells after 6 or 24 h of culture was quantified by MTT assay. The production of growth factors was normalized with the value of absorbance for reduced MTT. The recovered culture medium and the reduced MTT absorbance from cells cultured in scaffolds-free conditions were used as control. The results of viability and TGF-β1 secretion by macrophages seeded on wells before the addition of the materials into the culture wells showed a similar tendency to the obtained results when cells were directly seeded on materials (Figure S3).

Quantification of cytokines secreted by human monocytes/macrophages – Peripheral blood cells from healthy donors were separated by centrifugation (700 g, 30 min) on a two-phase density gradient of Histopaque 1077 and 1119 (SigmaAldrich, Mexico, cat 10771 and 11191). Peripheral blood mononuclear cells (monocytes/lymphocytes) were washed (sterile PBS, 3x) and centrifuged (700 g, 5 min). Then cells were suspended in RPMI medium supplemented with 10% FBS and antibiotics (50 μg mL^{-1} penicillin/streptomycin and 25 μg mL^{-1} amphotericin B) at a cell density of $8x10^5$ cells per mL, and plated to allow the adherence of monocytes. After 2 h, medium was removed in order to eliminate unattached cells. Antibiotics, FBS and macrophage colony stimulating factor (M-CSF, 30 pg mL^{-1}) were included in the renewed culture medium. Cells were allowed to differentiate for 9 days (37

°C, 5% CO_2), after which cells were re-plated every 7 days (3x) and then passed twice weekly (9x) by trypsinization (0.05% Trypsin-EDTA, Gibco®) and cultured with FBS and antibiotics but without M-CSF. Human macrophages differentiated from peripheral blood monocytes (12 passes after M-CSF induced differentiation) were plated at $35x10^3$ per well containing sterile glass slide in 24-well microplates and then cultured (10% FBS, 37°C, 5% CO_2, 95% humidity) for 16 h. Then sanitized ECM scaffolds (disks 15 mm) were placed in wells and the culture extended for 1, 2 or 4 days, after which medium was collected to quantify the cytokines. Quantification of the cytokines TGF-β1, TNF-α, IL-10 and IL-6 was performed using ELISA kits (eBioscience) according to specifications. The number of viable macrophages on the scaffolds and on the rest of the surface of the wells was quantified by MTT assay. The production cytokines by human macrophages was normalized with the value of absorbance for reduced MTT. The recovered culture medium and the reduced MTT absorbance from cells cultured in scaffolds-free conditions were used as control.

2.6 Statistical analysis

Data sets were compared using one-way analysis of variance (ANOVA). The Sidak-Holm Test was used for the comparison between data groups. The results were considered with statistically significant difference at *P*-values less than 0.05 and presented as mean ± standard deviation (SD). All the experiments were repeated independently at least three times.

3. Results

3.1. Silica incorporation on oligourethane/ECM and ECM scaffolds

The silica content in scaffolds was close to 1w% and 2w% for non-crosslinked ECM scaffold or oligourethane/ECM scaffolds, respectively (Fig 1a). SEM micrographs of sheets obtained after freeze-drying of hybrid scaffolds revealed silica particles deposited onto the ECM network (Fig. 1d and 1e). FT-IR spectra showed peaks at 1634 and 1555 cm^{-1}, attributed to amide I (C=O stretching) and II (N–H deformation) respectively, and 1078 and 787 cm^{-1}, attributed to (Si–O–Si) siloxane bonds (Fig. 1c). The effective deposition of silica particles onto the collagen fibrous network was resulted of the hydrolysis/polycondensation of sodium silicate catalyzed by hydrochloride acid under mild conditions and the subsequent freeze-drying.

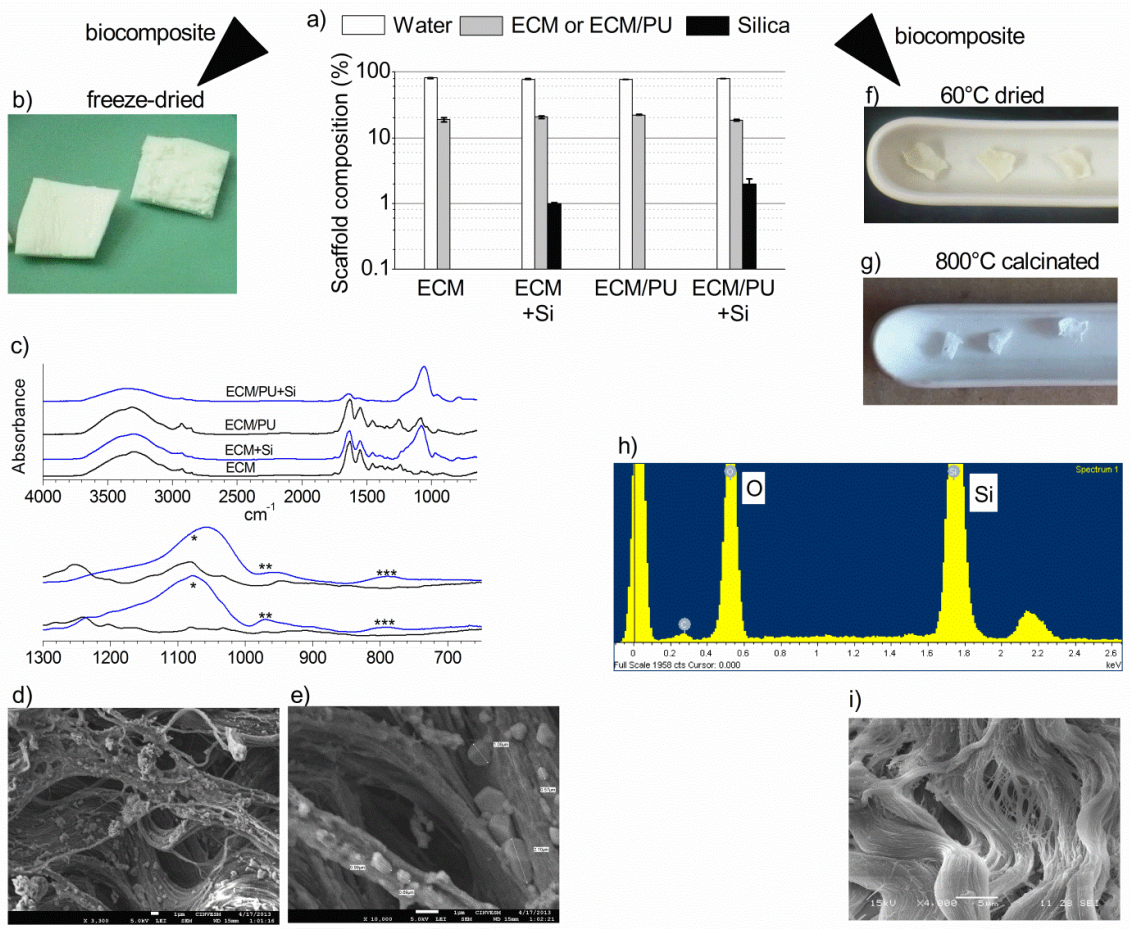

Figure 1

On the other hand, silicate-treated oligourethane/ECM or ECM materials dried at 60° (Fig 1f) and then calcinated at 800°C resulted in inorganic materials (Fig. 1g). The inorganic material that remains after calcination of hybrid scaffolds is composed mainly by silicon and oxygen as revealed by EDX analysis (Fig. 1h). At the same time, SEM analysis revealed a microstructure of the inorganic material that replicates the fibrous structure of the pericardial ECM scaffold (Fig. 1i).

3.2. Crosslinking density and water uptake of SiO_2-functionalized and oligourethane-crosslinked ECM scaffolds

The crosslinking degree and water uptake were investigated in order to establish how physicochemical characteristics would be affected by the composition of the biocomposites. DSC thermographs revealed an increment of denaturation temperature after crosslinking of ECM material with oligourethane (peak temperature from 66 to 82°C); however, this transition was no affected by silica incorporation (Fig. 2a). The content of residual scaffold-amines confirmed the crosslinking of ECM material with oligourethane to a degree of 91% of blocked amines (Fig 2b). After silica incorporation into the non-crosslinked ECM scaffolds close to 9% of amine groups were blocked without statistically significant differences with the ECM control (no silica).

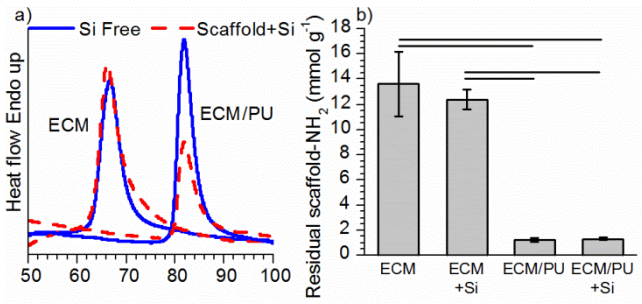

Figure 2

In presence of collagenase activity, silica-functionalized non-crosslinked ECM materials gained mass and elapsed its degradation time 1 to 2 days with respect to silica-free ECM scaffolds, whereas for oligourethane/ECM scaffolds, after 4 days, loss of mass was observed in silica-containing scaffolds without water uptake process (Fig. 3a). In presence of collagenase-free DMEM medium, non-crosslinked ECM scaffolds absorbed water until 7 days, after which the mass decreased, while for oligourethane/ECM scaffolds the water uptake ability was reduced (Fig. 3b). These results indicate that the enzymatic degradation of ECM scaffolds can be hindered by its crosslinking with oligourethane while the water uptake of ECM materials can be regulated by both its crosslinking with oligourethane and the incorporation of silica.

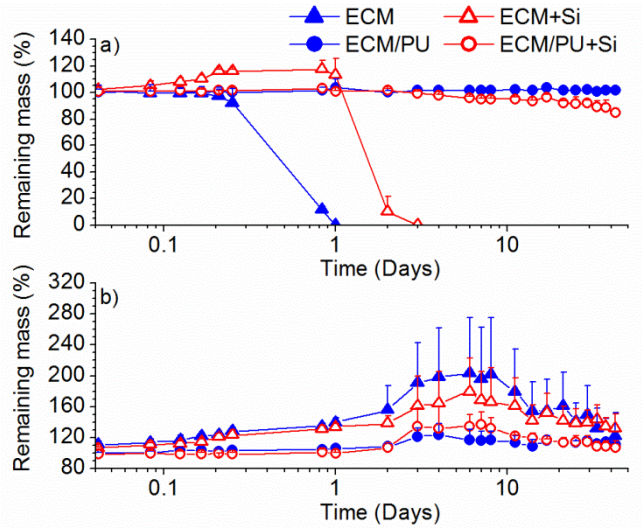

Figure 3

3.3. Cell viability on SiO_2-functionalized and oligourethane-crosslinked ECM scaffolds

In order to evaluate the effect of silica functionalization and the oligourethane crosslinking on the cytocompatibility of ECM scaffolds, cells were seeded directly on the lyophilized materials. The SEM micrographs revealed that the macrophages (Fig 4a-4b) and fibroblasts (Fig 4d-4e) spread on surface of scaffolds. Viable macrophage-like RAW264.7

line cells (Fig. 4c) and primary dermal fibroblasts (Fig. 4f) were detected on all four scaffolds by means of MTT assay. However, a reduction in the cell viability was detected on silica-containing scaffolds in both non-crosslinked and crosslinked. In addition, the viability measured on scaffolds was higher than the viability on the rest of the surface of polystyrene wells (Fig. 4c and 4f).

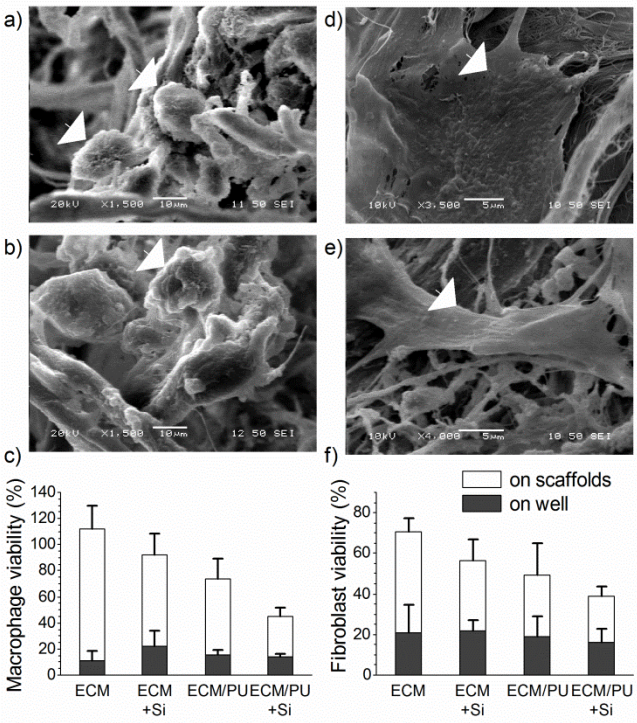

Figure 4

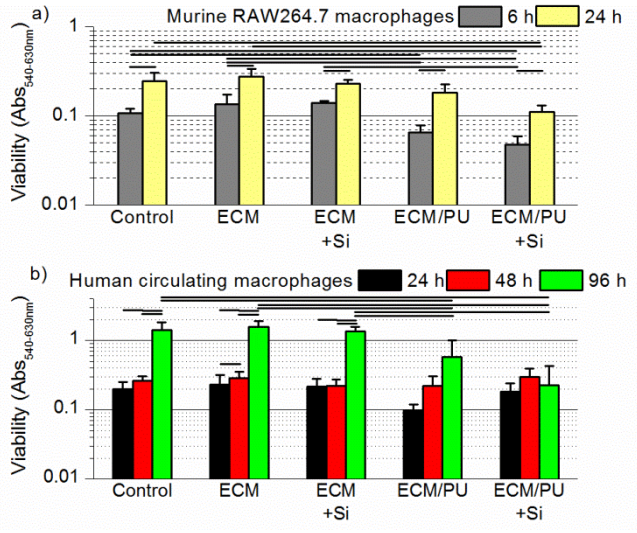

Figure 5

RAW264.7 macrophages and human blood macrophages were able to proliferate in the presence of all four scaffolds as evaluated by means of MTT reduction assay (Fig. 5a and 5b) and a fluorescent Live/Dead assay (Fig. 6a and 7a).

3.4. Angiogenic/fibrogenic growth factors secreted by RAW264.7 macrophages cultured on SiO_2-functionalized and oligourethane-crosslinked ECM scaffolds

To investigate if murine RAW264.7 macrophages respond to particulate silica and oligourethane crosslinker, the secretion of growth factors involved in angiogenesis and fibrogenesis processes was quantified when cells were cultured on the whole scaffolds. Macrophages cultured during 6 h, in contact with oligourethane/ECM and ECM scaffolds, secreted a higher amount of TGF-β1 (Fig. 6b), b-FGF (Fig. 6c) and VEGF (Fig. 6d) compared vs. control or vs. silica-containing scaffolds. Macrophage proliferation on oligourethane/ECM and ECM scaffolds from 6-to-24 h did not result in an increment of growth factors production, in fact, a drop in the secretion was observed. However, secretion of growth factors by RAW264.7 macrophages cultured in the presence of silica-containing scaffolds was not decreased with the culture time from 6-to-24 h.

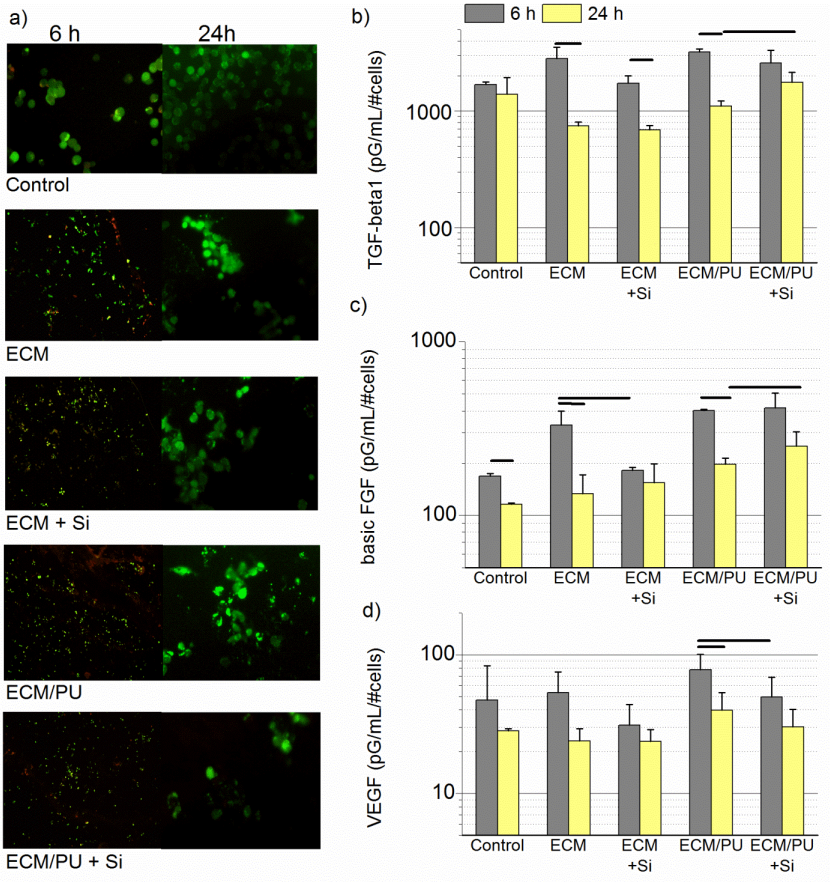

Figure 6

3.5. Cytokines secreted by human blood peripheral derived macrophages cultured on SiO_2-functionalized and oligourethane-crosslinked ECM scaffolds

The stimulation of primary human macrophages by particulate silica deposited on ECM scaffolds was investigated by means of the ability to elaborate cytokines involved in both, pro-inflammatory and anti-inflammatory process. The silica incorporation into the oligourethane/ECM and ECM scaffolds rendered a higher production of TNF-α (Fig. 7b), IL-6 (Fig. 7c) and IL-10 (Fig. 7e) by macrophages compared to silica-free scaffolds. In addition, a time-dependent decrease in the production of the three cytokine was detected. ECM scaffolds containing silica showed a minimal effect on TGF-β1 secretion and no time dependence (Fig 7d). Nonetheless, two different methods were used to active the TGF-β1,

i.e., to cleave the so called latency-associated peptide (LAP) from TGF-β1 protein, secreted by murine RAW264.7 and human-circulating macrophages, which represents a limitation in the quantification by ELISA of this signaling molecule (Fig. 6b and 7d). In fact, using the same protocol to generate the active form of TGF-β1, its secretion by murine and human macrophages was detected after 24 h of culture with scaffolds (Fig. S4).

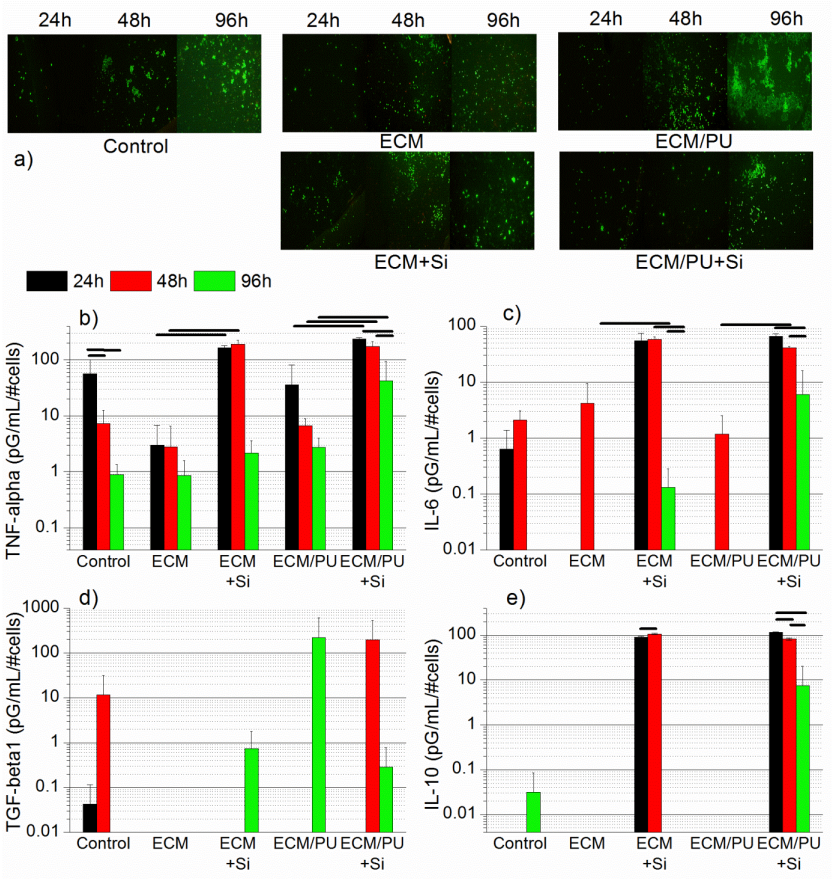

Figure 7

4. Discussion

An incorporation of bioactive molecules or a promotion of crosslinking in decellularized matrices offer a chance to enhance the physical and/or the biological performance by routes involving optimization of surface chemistry, regulation of biodegradation or controlled releasing of bioactive agents. Silica and its related degradation products impact the cell behavior which has shown some benefits for tissue engineering applications, for instance in the wound healing of chronic skin wounds [14] and in osteogenic differentiation of stem cells.[9-13] In the present study, we reported the functionalization of crosslinked or non-crosslinked ECM scaffolds with particulate silica by hydrolysis/polycondensation of sodium silicate, and the release of certain soluble signaling molecules by macrophages when cultured in the presence of scaffolds functionalized with silica.

The neutralization of sodium silicate solution induces the gelation typically rather quickly by a single step process. After neutralization of Na_4SiO_4 solution with HCl, the polymerization of orthosilicic acid in presence of ECM materials allowed a homogenous incorporation of silica hydrogel as result of the formation of colloidal silica into aggregates. Silica aggregates occupied interstitial spaces of decellularized pericardial matrix. Another important point to mention is that ECM materials containing silica hydrogel served as a template in the generation of silica material that mimics the microstructure of fibrous tissue because of the polymerization of silica during the calcination (Fig. 1g-1i). On the other hand, the freeze-drying of ECM materials containing silica hydrogel induced the deposition of silica particles onto the fibrous collagen (Fig. 1d-1e). The oligourethane/ECM and ECM materials functionalized with silica particles were chosen to investigate the effect of silica on the stability, *in vitro* degradation and macrophages response.

The increase of the ECM scaffold stability, as evidenced by the increases of collagen denaturation temperature (Fig. 2a), the decreases of free collagen-amines (Fig. 2b) and the

resistance to collagenase degradation (Fig. 3a), was produced by the crosslinking with oligourethane and was not affected by the incorporation of particulate silica. The silica inside interstitial spaces in the ECM material can confer an enhanced water uptake process in silica-ECM scaffolds (Fig. 3a). By contrast, for crosslinked-ECM scaffolds, the reduced interstitial spaces can hinder the water uptake (Fig. 3a-3b). All these results indicated an effective incorporation of silica into the ECM scaffolds both, non-crosslinked and oligourethane-crosslinked.

To have a first idea of the effect of the silica incorporation into the ECM scaffolds on biocompatibility, we measured the viability of dermal fibroblast and RAW264.7 macrophages cultured on scaffolds. The cells adhered and viable onto silica-ECM scaffolds were revealed by SEM micrographs (Fig. 4a-4b and 4d-4e) and MTT reduction assay, respectively. The drop of the viability of cells after crosslinking (Fig. 4c, 4f) can be induced by a masking of focal adhesion sites on the collagen network of the decellularized scaffolds. In addition, a drop in the viability of cells was observed on scaffolds functionalized with silica compared to silica-free scaffolds (Fig. 4c, 4f). The impact of silica on viability of macrophages and fibroblasts can be a result of the interaction between cells and particles on the ECM material. The silica particles and its dissolution products after internalization can disturb the networks that maintain homeostasis during proliferation, differentiation, and apoptosis. [47] The reactive oxygen species generated in cells stimulated with different particles is considered a major factor in particle-induced cytotoxicity. [47-48]

In previous studies, it has been reported that silica biomaterials are able to modify the cell behavior. [6,29-30] Hence, silica-ECM hybrid scaffolds is a suitable platform to characterize the cellular response to biocomposites that release silicon species. Macrophages are cells of the innate immune system with a dominant effector activity in the injury site after biomaterial implantation. [38] Cross-talk between immune cells activates macrophages after which, they release a variety of signaling molecules. Signaling molecules secreted by macrophages such

as cytokines (as interleukins), growth factors (as b-FGF, VEGF), TGF-β1 and TNF-α influence the development of other cell types. [44-45] In fact, the profile of signaling molecules secretion is commonly evaluated to study the polarization of the macrophage response from an inflammation and tissue injury process to a repair process [36] or to study angiogenesis and scaffold vascularization. [45]

Macrophages showed the ability to proliferate on all scaffolds, including those that contain particulate silica (Fig 5a, 5b, 6a and 7a). The secretion of growth factors by RAW264.7 macrophages in a sustained manner (Fig. 6b-6d) and interleukins by human macrophages in up-regulated manner (Fig. 7b-7e) when cells were cultured with silica-ECM scaffolds suggests that silica debris induces the activation of macrophages. Debris of the silica particles incorporated on ECM scaffolds can be internalized by macrophages, as previously reported after culture of HepG2 epithelial-like cells [49] and human endothelial cells [50] with silica nanoparticles. An internalization of silica compounds by macrophages can further influence signaling pathways to increase the production of signaling molecules. The macrophages activation with silica nanoparticles has been promoted to assist the DNA vaccination in the treatment of infectious diseases. [24] The interaction of stem cells with silica nanoplatelets has induced the osteogenic differentiation. [51] Since the hydrolysis of silicate materials occurs in aqueous solution under mild conditions, biodegradation products of silica can be related with the impact of silica on cell response. Porous sol–gel silica particles have been biodegraded in culture media [52] and under physiological flow conditions [53] by hydrolysis or dissolution to form orthosilicic acid, $Si(OH)_4$. [54] In fact, stimulation of human skin cells guided by the release of high molecular weight decomposition products from silicon-based biodegradable inorganic material has been related with the regulation of wound healing. [14] The incorporation of silica into biodegradable scaffolds has proven to be an effective strategy to induce the formation of hydroxyapatite on scaffolds [10,55] while allows the growth of osteoblasts and moderate release of H_2O_2 by macrophages. [10] A rapid and robust angiogenic

response in a quail chorioallantoic membrane model has been supported by collagen films functionalized with bioglass that contain silicon. [35] The *in vitro* cytotoxicity and expression of pro-inflammatory cytokines by macrophages has been reduced by stimulation with mesoporous silica nanoparticle unlike colloidal silica nanoparticles. [56] Along with these previous findings, stimulation of macrophages induced by silica particles *in situ* deposited onto the ECM network can be explored in the *in vitro* strategies that combine cell co-culture [44,57] or exogenous stimulating factors [45,58-59] in order to promote the biological response to ECM biomaterials in different tissue engineering applications. Considering that bone-related cell lines have showed responsiveness towards silica to maintain the morphogenetic stimuli of silica on 2D or 3D cultures [60-61], the series of silica-decellularized tissue composites can offer a suitable template for enhanced osteogenic potential while the *in vivo* biodegradation is adjusted by the crosslinking, which is a subject of ongoing research.

5. Conclusions

Particulate silica was effectively incorporated into the decellularized tissue scaffolds either non-crosslinked or crosslinked by isocyanate chemistry. The stability and water uptake of the biocomposites were reliant on crosslinking but were not reliant on the incorporation of silica. Murine RAW264.7 macrophages cultured on ECM materials crosslinked with oligourethane and functionalized with silica were able to secrete b-FGF, TGF-β1 and VEGF. Secretion of growth factors by RAW264.7 macrophages after 6 h of culture on scaffolds containing silica was lower but it was sustained for 24 h as compared to cells cultured on silica-free materials. The secretion of IL-6, IL-10 and TNF-α by human macrophages was increased with the presence of scaffolds containing silica and it was decreased in a time-dependent manner from one to four days of culture.

Acknowledgements: We thank to Julio C. Martínez and Mayra C. Rodríguez (UG) for technical assistance with fibroblast culture and to Rossana F. Vargas and Prof. Juan V. Cauich (*Centro de Investigación Científica de Yucatán*) for technical assistance and facilities with SEM and DSC analyses. GGG thanks to MC Dora A. Huerta Q. for technical assistance with SEM analysis at LANNBIO Cinvestav-unidad Mérida Yucatán. This research was supported by the *Consejo Nacional de Ciencia y Tecnología* (México) through the project CB2011/164440 and the Fund *Convocatoria Interinstitucional CIO-UG 2013*.

References

1 S. Rajabi-Zeleti, S. Jalili-Firoozinezhad, M. Azarnia, F. Khayyatan, S. Vahdat, S. Nikeghbalian, A. Khademhosseini, H. Baharvand and N. Aghdami, *Biomaterials,* 2014, **35**, 970.

2 B. N. Brown, R. Londono, S. Tottey, L. Zhang, K. A. Kukla, M. T. Wolf, K. A. Daly, J. E. Reing and S. F. Badylak. *Acta Biomater*., 2012, **8**, 978.

3 B. Mendoza-Novelo, D. I. Alvarado-Castro, J. L. Mata-Mata, J. V. Cauich-Rodríguez, A. Vega-González, E. Jorge-Herrero, F. J. Rojo and G. V. Guinea, *Mater. Sci. Eng. C*, 2013, **33**, 2392.

4 B. Mendoza-Novelo, J. L. Mata-Mata, A. Vega-González, J. V. Cauich-Rodríguez and A. Marcos-Fernández, *J. Mater. Chem. B,* 2014, **2**, 2874.

5 B. Mendoza-Novelo, G. González-García, J. L. Mata-Mata, L. E. Castellano, P. Cuéllar-Mata and E. E. Ávila, *Mater. Letters*, 2013, **106**, 369.

6 A.M. Mebert, D. E. Camporotondi, M. L. Foglia, G. S.Alvarez, P. L. S. Orihuela, L. E. Diaz and M. F. Desimone, *J. Biomater. Tissue Eng*., 2013, **3**, 108.

7 K. Rezwan, Q. Z. Chen, J. J. Blaker and A. R. Boccaccini, *Biomaterials*, 2006, **27**, 3413.

8 K. H. Lee and S. H. Rhee., *Biomaterials*, 2009, **30**, 3444.

9 C. Wu, W. Fan, J. Chang and Y. Xiao, *J. Mater. Chem*., 2011, **21**, 18300.

10 W. Zhai, H. Lu, C. Wu, L. Chen, X. Lin, K. Naoki, G. Chen and J. Chang, *Acta Biomater.*, 2013, 9, 8004.

11 W. E. G. Müller, X. Wang, V. Grebenjuk, B. Diehl-Seifert, R. Steffen, U. Schloßmacher, A. Trautwein, S. Neumann and H. C. Schröder, *Biomater. Sci.*, 2013, **1**, 669.

12 A. I. Rodrigues, M. E. Gomes, I. B. Leonor and R. L. Reis, *Acta Biomater.*, 2012, **8**, 3765.

13 G. Tomoaia, A. Mocanu, I. Vida-Simiti, N. Jumate, L. D. Bobos, O. Soritau and M. Tomoaia-Cotisel, *Mater. Sci. Eng. C*, 2014, **37**, 37.

14 V. Grotheer, M. Goergens, P. C. Fuchs, S. Dunda, N. Pallua, J. Windolf and C. V. Suschek, *Biomaterials*, 2013, **34**, 7314.

15 M. F. Desimone, C. Hélary, I. B. Rietveld, I. Bataille, G. Mosser, M. M. Giraud-Guille, J. Livage and T. Coradin, *Acta Biomater*., 2010, **6**, 3998.

16 U. Schloßmacher, H. C. Schröder, X. Wang, Q. Feng, B. Diehl-Seifert, S. Neumann, A. Trautweina and W. E. G. Müller, *RSC Adv.*, 2013, **3**, 11185.

17 A. Angelopoulou, E. K. Efthimiadou and G. Kordas, *Mater Lett*., 2012, **74**, 50.

18 P. C. Balaurea, E. Andronescu, A. M. Grumezescu, A. Ficai, K. S. Huang, C. H. Yang, C. M. Chifiriuc and Y. S. Lin, *Int. J. Pharm.*, 2013, **441**, 555.

19 F. Tang, L. Li and D. Chen, *Adv. Mater*., 2012, **24**, 1504.

20 M. Colilla, B. González and M. Vallet-Regí, *Biomater. Sci*., 2013, **1**, 114.

21 G. S. Alvarez, C. Hélary, A. M. Mebert, X. Wang, T. Coradin and M. F. Desimone, *J. Mater. Chem. B*, 2014, **2**, 4660.

22 F. M. Chen, M. Zhang and Z. F. Wu, *Biomaterials*, 2010, **31**, 6279.

23 S. Chen, A. Osaka, T. Ikoma, H. Morita, J. Li, M. Takeguchi and N. Hanagata, *J. Mater. Chem*., 2011, **21**, 10942.

24 J. Wang, R. Zhu, B. Gao, B. Wu, K. Li, X. Sun, H. Liu and S. Wang, *Biomaterials* 2014, **35**, 466.

25 X. Wang, X. Li, A. Ito, Y. Sogo and T. Ohno, *Acta Biomater*. 2013, **9**, 7480.

26 Y. Shirosaki, K. Tsuru, S. Hayakawa, A. Osaka, M. A. Lopes, J. D. Santos and M. H. Fernandes, *Biomaterials*, 2005, **26**, 485.

27 L. Ren, K. Tsuru, S. Hayakawa and A. Osaka, *J. Non-Cryst. Solids*, 2001, **285**, 116.

28 H. Zhang, D. R. Dunphy, X. Jiang, H. Meng, B. Sun, D. Tarn, M. Xue, X. Wang, S. Lin, Z. Ji, R. Li, F. L. Garcia, J. Yang, M. L. Kirk, T. Xia, J. I. Zink, A. Nel and C. J. Brinker, *J. Am. Chem. Soc*., 2012, **134**, 15790.

29 P. Han, C. Wu and Y. Xiao, *Biomater. Sci*., 2013, **1**, 379.

30 A. Hoppe, N. S. Güldal and A. R. Boccaccini, *Biomaterials*, 2011, **32**, 2757.

31 H. S. Yun, J. W. Park, S. H. Kim, Y. J. Kim and J. H. Jang, *Acta Biomater*., 2011, **7**, 2651.

32 J. Kasper, M. I. Hermanns, C. Bantz, O. Koshkina, T. Lang, M. Maskos, C. Pohl, R. E. Unger and C. J. Kirkpatrick, *Arch. Toxicol*., 2013, **87**, 1053.

33 Z. Mao, X. Zhou and C. Gao, *Biomater. Sci.*, 2013, **1**, 896.

34 S. Quignard, G. Mosser, M. Boissière and T. Coradin, *Biomaterials*, 2012, **33**, 4431.

35 G. E. Vargas, L. A. H. Durand, V. Cadena, M. Romero, R. V. Mesones, M. Mackovic, S. Spallek, E. Spiecker, A. R. Boccaccini and A. A. Gorustovich, *J. Mater. Sci. Mater. Med*., 2013, **24**, 1261.

36 S. Quignard, C. Hélary, M. Boissière, J. M. Fullana, P. Y. Lagrée and T. Coradin, *Biomater. Sci.*, 2014, **2**, 484.

37 S. Franz, S. Rammelt, D. Scharnweber and J. C. Simon, *Biomaterials*, 2011, **32**, 6692.

38 M. Jaguin, N. Houlbert, O. Fardel and V. Lecureur, *Cellular Immunol*., 2013, **281**, 51.

39 V. Ballotta, A. Driessen-Mol, C. V. C. Bouten and F. P. T. Baaijens, *Biomaterials*, 2014, **35**, 4919.

40 J. Maciel, M. I. Oliveira, R. M. Gonçalves and M. A. Barbosa, *Acta Biomater*., 2012, **8**, 3669.

41 J. Kajahn, S. Franz, E. Rueckert, I. Forstreuter, V. Hintze, S. Moeller and J. C. Simon, *Biomatter* 2012, **2**, 226.

42 M. B. Ariganello, D. T. Simionescu, R. S. Labowa and J. M. Lee, *Biomaterials*, 2011, **32**, 439.

43 R. M. Day and A. R. Boccaccini, *J. Biomed. Mater. Res. A*, 2005, **73**, 73.

44 E. Dohle, I. Bischoff, T. Böse, A. Marsano, A. Banfi, R. E. Unger and C. J. Kirkpatrick, *Eur. Cell. Mater*., 2014, **27**, 149.

45 K. L. Spiller, R. R. Anfang, K. J. Spiller, J. Ng, K. R. Nakazawa, J. W. Daulton and G. Vunjak-Novakovic, *Biomaterials*, 2014, **35**, 4477.

46 B. Mendoza-Novelo, E. E. Avila, J. V. Cauich-Rodríguez, E. Jorge-Herrero, F. J. Rojo, G. V. Guinea and J. L. Mata-Mata, *Acta Biomater*., 2011, **7**, 1241.

47 Q. Mu, G. Jiang, L. Chen, H. Zhou, D. Fourches, A. Tropsha and B. Yan, *Chem. Rev.*, 2014, **114**, 7740.

48 T. Xia, M. Kovochich, J. Brant, M. Hotze, J. Sempf, T. Oberley, C. Sioutas, J. I. Yeh, M. R. Wiesner and A. E. Nel, *Nano Lett*., 2006, **6**, 1794.

49 L. Hu, Z. Mao, Y. Zhang and C. Gao, *J. Nanosci. Lett*., 2011, **1**, 1.

50 W. Zhai, C. He, L. Wu, Y. Zhou, H. Chen, J. Chang and H. Zhang, *J. Biomed. Mater. Res. B Appl. Biomater*., 2012, **100**, 1397.

51 A. K. Gaharwar, S. M. Mihaila, A. Swami, A. Patel, S. Sant, R. L. Reis, A. P. Marques, M. E. Gomes and A. Khademhosseini, *Adv. Mater*., 2013, **25**, 3329.

52 M. Cicuéndez, P. Portolés, M. Montes-Casado, I. Izquierdo-Barba, M. Vallet-Regí, and M.T. Portolés, *J. Mater. Chem. B*, 2014, **2**, 3469.

53 Q. He, J. Shi, M. Zhu, Y. Chen and F. Chen, *Micropor. Mesopor. Mater.*, 2010, **131**, 314.

54 T. Coradin, D. Eglin and J. Livage, *Spectroscopy*, 2004, **18**, 567.

55 C. E. Plazas Bonilla, S. Trujillo, B. Demirdögen, J. E. Perilla, Y. M. Elcin and J. L. Gómez Ribelles, *Mater. Sci. Eng. C*, 2014, **40**, 418.

56 S. Lee, H. S. Yun and S. H. Kim, *Biomaterials*, 2011, **32**, 9434.

57 K. G. Battiston, J. W. C. Cheung, D. Jain and J. P. Santerre, *Biomaterials*, 2014, **35**, 4465.

58 R. Augustine, E. A. Dominic, I. Reju, B. Kaimal, N. Kalarikkal and S. Thomas, *RSC Adv.*, 2014, **4**, 51528.

59 Y. Rong, T. Zhou, W. Cheng, J. Guo, X. Cui,Y. Liu and W. Chen, *Environ. Toxicol. Pharmacol.* 2013, **36**, 921.

60 T. Link, X. Wang, U. Schloßmacher, Q. Feng, H. C. Schröder and W. E. G. Müller, *RSC Adv.*, 2013, **3**, 11140.

61 M. Wiens, X. Wang, H. C. Schröder, U. Kolb, U. Schloßmacher, H. Ushijima and W. E. G. Müller, *Biomaterials*, 2010, **31**, 7716.

Figure captions:

Figure 1. a) Content of silica, oligourethane(PU)/ECM or ECM material and water for biocomposites (n=4). Representative b) photographs (after freeze-drying), c)ATR-FTIR spectra, d) and e) SEM micrographs, f) photographs (after dry 60°C), g) photographs (after calcination 800°C) of the biocomposites. Representative h) EDX spectrum and i) SEM micrograph of silica material (see Fig. 1g) that remains calcination process.

Figure 2. a) DSC thermographs and b) free ECM material-amines for hydrated materials: ECM – uncrosslinked materials, ECM/PU – materials crosslinked with oligourethane, Si – materials functionalized with particulate silica; n=3; statistically significant differences for marked groups.

Figure 3. Water uptake /degradation behavior evaluated by means of loss/gain of mass in the presence of a) collagenase type I and b) DMEM medium for the freeze-dried materials: ECM – uncrosslinked materials, ECM/PU – materials crosslinked with oligourethane, Si – materials functionalized with particulate silica; n=3.

Figure 4. Representative SEM micrographs of RAW264.7 macrophages seeded on a) ECM scaffolds and b) silica-ECM scaffolds and fibroblasts seeded on d) ECM scaffolds and e) silica-ECM scaffolds. Viability of c) macrophages and f) fibroblasts assessed by MTT reduction by cells on freeze-dried materials (ECM – uncrosslinked materials, ECM/PU – materials crosslinked with oligourethane, Si – materials functionalized with particulate silica) and polystyrene wells after 24 h of culture. 100% represent viability of cells proliferating on polystyrene wells free of materials; n=4.

Figure 5. Viability of a) RAW264.7 macrophages and b) human macrophages assessed by MTT reduction by cells on freeze-dried materials (ECM – uncrosslinked materials, ECM/PU – materials crosslinked with oligourethane, Si – materials functionalized with particulate silica). Control – cells proliferating on polystyrene wells free of materials; n=4; statistically significant differences for all marked groups.

Figure 6. a) Representative fluorescent micrographs for RAW264.7 macrophages proliferating for 6 and 24 h on freeze-dried materials. Growth factor secretion analysis from RAW264.7 macrophages for b) TGF-β1, c) b-FGF and d) VEGF after 6 and 24 h of culture on freeze-dried materials (ECM – uncrosslinked materials, ECM/PU – materials crosslinked with oligourethane, Si – materials functionalized with particulate silica). Control – cells proliferating on polystyrene wells free of materials; n=3; statistically significant differences for all marked groups.

Figure 7. a) Representative fluorescent micrographs for human peripheral blood derived macrophages proliferating for 1, 2 and 4 days on freeze-dried materials. Cytokine secretion

analysis from human macrophages for b) TNF-α, c) IL-6, d) TGF-β1, d) IL-10 after 1, 2 or 4 day of culture on freeze-dried materials (ECM – uncrosslinked materials, ECM/PU – materials crosslinked with oligourethane, Si – materials functionalized with particulate silica). Control – cells proliferating on polystyrene wells free of materials; n=3; statistically significant differences for all marked groups.